J Musculoskelet Neuronal Interact 2026; 26(2):285-292

Journal of Musculoskeletal and Neuronal Interactions JMNI

Original Article

Expression of miR-27a in Patients with Steroid-associated Femoral Head Osteonecrosis and Its Regulatory Mechanism on Proliferation and Osteogenic Differentiation of Bone Marrow Mesenchymal Stem Cells

Zhiqing Chen[#1,2,3,4,5], Min Wang[#6], Zepei Zhang[7], Chun Zhang[2,3,4,5], Yuzhe Cao[2,3,4,5], Shaoming Liu[2,3,4,5], Shuzhang Guo[2,3,4,5], Jun Miao[7]

[1]Clinical College of Orthopedics, Tianjin Medical University, China;
[2]Department of Orthopedics, The Third Central Hospital of Tianjin, Tianjin, China;
[3]Tianjin Key Laboratory of Extracorporeal Life Support for Critical Diseases, Tianjin, China;
[4]Artificial Cell Engineering Technology Research Center, Tianjin, China;
[5]Tianjin Institute of Hepatobiliary Disease, Tianjin, China;
[6]Department of Orthopedics (Spine Division), Beichen Hospital Affiliated to Nankai University, Tianjin, China;
[7]Department of Spine Surgery, Tianjin Hospital, Tianjin University, Tianjin, China
[#]Equal Contribution

Abstract

Objectives: To investigate the expression of microRNA-27a (miR-27a) in patients with steroid-associated femoral head osteonecrosis (SAN) and its regulatory effects on bone marrow mesenchymal stem cells (BMSCs). **Methods**: The expression levels of miR-27a and the osteogenic-related genes Runt-related transcription factor 2 (Runx2) and bone morphogenetic protein 2 (BMP-2) were measured in bone marrow samples from SAN patients and controls. Human BMSCs were cultured *in vitro* and divided into four groups: blank control group, mimic negative control (mimic NC) group, miR-27a mimic group, and miR-27a inhibitor group. Cell proliferation, osteogenic differentiation, and expression of osteogenic-related genes were assessed. **Results**: The relative expression levels of miR-27a, Runx2, and BMP-2 in bone marrow tissues of the SAN group were significantly lower than those in the control group (all $P<0.001$). miR-27a expression was positively correlated with Runx2 and BMP-2 expression ($P<0.001$). Compared with the mimic NC group, the miR-27a mimic group showed increased cell proliferation (OD values), alkaline phosphatase (ALP) activity, number of calcium nodules, and expression levels of Runx2 and BMP-2 (all $P<0.05$). Compared with the mimic NC group, the miR-27a inhibitor group showed significantly decreased cell proliferation (OD values), ALP activity, number of calcium nodules, and expression levels of Runx2 and BMP-2 (all $P<0.05$). **Conclusion**: miR-27a may promote the proliferation and osteogenic differentiation of BMSCs by upregulating Runx2 and BMP-2 and may represent a potential therapeutic target for the treatment of SAN.

Keywords: Bone Marrow Mesenchymal Stem Cells, Cell Proliferation, miR-27a, Osteogenic Differentiation, Steroid-associated Femoral Head Osteonecrosis

Introduction

Femoral head necrosis is a common and refractory orthopedic disease characterized by interruption or damage of the blood supply to the femoral head. This leads to death of osteocytes and bone marrow components, structural changes, and eventual collapse of the femoral head. Among the etiologies, steroid-associated femoral

The authors have no conflict of interest.

Corresponding author: Jun Miao, Department of Spine Surgery, Tianjin Hospital, Tianjin University, No. 406 Jiefang South Road, Hexi District, Tianjin 300299, China
E-mail: Miaojun_tj2026@163.com

Edited by: G. Lyritis
Accepted 10 February 2026

head osteonecrosis (SAN) has accounted for an increasing proportion of clinical cases in recent years, severely affecting patients' quality of life and limb function[1,2]. Long-term or high-dose glucocorticoid use is the primary risk factor for SAN; however, its specific pathogenesis remains incompletely understood. Current evidence suggests that impaired proliferation and osteogenic differentiation of bone marrow mesenchymal stem cells (BMSCs) play a critical role in disease progression[3].

MicroRNAs (miRNAs) are a class of endogenous non-coding RNAs approximately 22 nucleotides in length that play important roles in bone metabolism and skeletal diseases[4,5]. As a member of the miRNA family, miR-27a has been shown to participate in the pathological processes of various diseases, regulating cell proliferation, angiogenesis, and adipocyte differentiation, particularly in tumor cells[6].

Recent studies have suggested a potential association between miR-27a and bone metabolism. For example, in osteoblast differentiation models, miR-27a can target and inhibit negative regulators, thereby promoting the expression of osteogenic markers[7]. However, the expression pattern of miR-27a in SAN patients and its specific regulatory mechanisms on BMSC proliferation and osteogenic differentiation remain unclear.

Therefore, this study aimed to investigate the expression level of miR-27a in the bone marrow tissue of SAN patients, to explore its effects on BMSC proliferation and osteogenic differentiation through *in vitro* cell experiments, and to preliminarily elucidate the underlying mechanisms. These findings may provide experimental evidence for clarifying the pathogenesis of SAN and lay a foundation for identifying new therapeutic targets.

Materials and Methods

Clinical Data

We performed a retrospective observational study. A total of 80 patients diagnosed with SAN who visited The Third Central Hospital of Tianjin between March 2024 and March 2025 were enrolled as the case group.

Diagnostic criteria for SAN

(1) A clear history of high-dose corticosteroid use, with an average daily dose ≥16.6 mg or a maximum daily dose ≥80 mg for at least 1 year;
(2) Confirmation by MRI, with imaging features including bone marrow edema and signal changes in the weight-bearing area of the femoral head (low signal on T1WI and high signal on T2WI or a "linear sign"). Some patients also had bone density changes on CT.

Inclusion criteria: meeting the diagnostic criteria for SAN; age 30–66 years; no history of hip surgery; and voluntary participation in this study with signed informed consent.

Exclusion criteria: concomitant bone metabolic disorders (e.g., hyperparathyroidism); recent use (within 3 months) of medications affecting bone metabolism; or severe systemic diseases (e.g., cardiac, hepatic, or renal dysfunction).

During the same period, 80 patients undergoing elective orthopedic surgery (e.g., for lumbar disc herniation or postoperative lower-limb fracture management) at our hospital were selected as the control group. These control patients met the same exclusion criteria as the case group (no history of long-term or high-dose steroid use, no bone metabolic disorders, and no severe systemic diseases), ensuring comparability with respect to major confounding factors.

In the case group, there were 45 males and 35 females, aged 32–65 years (mean ± standard deviation [$\bar{x}\pm s$]: 48.25±8.12 years). In the control group, there were 43 males and 37 females, aged 30–66 years ($\bar{x}\pm s$: 47.86±7.95 years). There were no statistically significant differences in sex or age between the two groups ($P>0.05$), indicating good comparability.

SAN patients in the case group were staged using the ARCO (Association Research Circulation Osseous) system: 12 cases in stage I, 35 in stage II, 28 in stage III, and 5 in stage IV; 52 patients had unilateral involvement and 28 had bilateral involvement. Underlying diseases in the case group were as follows: 23 cases of systemic lupus erythematosus, 18 of rheumatoid arthritis, 15 of nephrotic syndrome, and 24 of other conditions. The cumulative steroid dose was 3852.6±1256.3 mg, the peak steroid dose was 65.84±18.58 mg/d, and the duration of steroid treatment was 18.63±7.21 months.

The primary indications for surgery in the control group were lumbar disc herniation (32 cases), postoperative lower-limb fractures (28 cases), and other conditions (20 cases).

Method of obtaining bone marrow samples:

(1) **Case group**: All patients underwent hip core decompression surgery. Bone marrow samples (approximately 2–3 mL) were collected from the necrotic area of the proximal femoral head.
(2) **Control group**: During elective orthopedic surgery, bone marrow samples (approximately 2–3 mL) were collected from the iliac crest.

All sampling procedures were performed under anesthesia using strict aseptic technique. Standard hemostasis and anti-infection measures were implemented after surgery to ensure patient safety. The collected bone marrow samples were immediately frozen in liquid nitrogen for subsequent detection of miR-27a and related gene expression levels.

Experimental Cells

Bone marrow mesenchymal stem cells (BMSCs) were purchased from the China Center for Type Culture Collection (CCTCC; catalog number CCTC-C1998001, batch number 202402). Cells were cultured in low-glucose Dulbecco's modified Eagle's medium (DMEM) supplemented with 10%

fetal bovine serum (FBS) and 1% penicillin–streptomycin (pen–strep) at 37°C in a humidified incubator with 5% CO_2. When cell confluence reached 80%–90%, cells were digested with 0.25% trypsin and subcultured.

Cell identity was verified based on the identification report provided by the supplier: the cells expressed mesenchymal surface markers CD29, CD44, and CD90, with positivity ≥95%, and did not express hematopoietic stem cell markers CD34 and CD45, with positivity ≤2%, which is consistent with the biological characteristics of BMSCs.

Main reagents and instruments

Reagents

FBS, low-glucose DMEM, 0.25% trypsin, and pen–strep were purchased from Gibco (USA). The miR-27a mimic (catalog number miR1000799-1-5), miR-27a inhibitor (catalog number miR2000799-1-5), mimic NC (catalog number miR1N0000001-1-5) were purchased from Guangzhou Ruibo Biotechnology Co., Ltd. (China). The miR-27a mimic sequence was 5'-AAGUGUCACCGAUUCAAGGCG-3', and the miR-27a inhibitor sequence was 5'-GCGGAACUUAGCCACUGUGAA-3'. The mimic NC sequence was 5'-UUCUCCGAACGUGUCACGUTT-3'. Lipofectamine 3000 transfection reagent was obtained from Invitrogen (USA). RNA extraction kits, reverse transcription kits, and SYBR Green PCR Master Mix were purchased from TaKaRa (Japan). Alkaline phosphatase (ALP) staining and alizarin red staining kits were obtained from Solarbio Technology Co., Ltd. (Beijing, China). The CCK-8 cell proliferation assay kit was obtained from Dojindo (Japan).

Instruments

A CO_2 incubator (Thermo Fisher Scientific, USA), super clean bench (Suzhou Purification Equipment Co., Ltd., China), inverted microscope (Olympus, Japan), ABI 7500 real-time PCR system (Applied Biosystems, USA), and microplate reader (Bio-Rad, USA) were used in this study.

Detection of miR-27a and related gene expression levels

Total RNA was extracted from bone marrow tissue samples (case and control groups) and from cultured BMSCs using an RNA extraction kit. cDNA was synthesized from RNA using a reverse transcription kit. The reverse transcription reaction conditions were: 37 °C for 15 minutes, 85 °C for 5 seconds, followed by storage at 4 °C.

Quantitative real-time PCR (qRT-PCR) was performed using SYBR Green PCR Master Mix on an ABI 7500 real-time PCR system to detect the expression levels of miR-27a, Runx2, and BMP-2. U6 and GAPDH were used as internal controls, and relative gene expression levels were calculated using the $2^{-\Delta\Delta Ct}$ method. Specifically, U6 was used as the internal control for miR-27a, and GAPDH was used as the internal control for Runx2 and BMP-2.

Primer sequences were as follows:

- **miR-27a:**
  - o Forward (F): 5'-ATATGAGAAAAGAGCTTCCCTGTG-3'
  - o Reverse (R): 5'-CAAGGCCAGAGGAGGTGAG-3'
- **Runx2:**
  - o Forward (F): 5'-CTTTACTTACACCCCGCCAGTC-3'
  - o Reverse (R): 5'-AGAGATATGGAGTGCTGGTC-3'
- **BMP-2:**
  - o Forward (F): 5'-AGTTCTGTCCCCAGTGACGAGTTT-3'
  - o Reverse (R): 5'-GTACAACATGGAGATTGCGCTGAG-3'
- **U6 (internal control for miR-27a):**
  - o Forward (F): 5'-CTCGCTTCGGCAGCACA-3'
  - o Reverse (R): 5'-AACGCTTCACGAATTTGCGT-3'
- **GAPDH (internal control for Runx2 and BMP-2):**
  - o Forward (F): 5'-GGAGCGAGATCCCTCCAAAAT-3'
  - o Reverse (R): 5'-GGCTGTTGTCATACTTCTCATGG-3'

Transfection of BMSCs

BMSCs in the logarithmic growth phase were seeded into 6-well plates at a density of 2×105 cells per well. When cell confluence reached 50%–60%, transfection was performed according to the Lipofectamine 3000 protocol. The final concentrations of all transfected oligonucleotides were 50 nmol/L. The volume ratio of Lipofectamine 3000 to RNA was 2:1 (μL:μg).

Cells were divided into four groups:

- **Blank control group**: untransfected BMSCs cultured under standard conditions;
- **Mimic NC group**: transfected with the miRNA mimic negative control sequence;
- **miR-27a mimic group**: transfected with miR-27a mimics for overexpression;
- **miR-27a inhibitor group**: transfected with miR-27a inhibitors for knockdown.

The blank control group was used as a qualitative reference for staining experiments and was not included in the subsequent quantitative statistical analyses. After 6 hours of transfection, the medium was replaced with fresh complete culture medium. Subsequent experiments were conducted 48 hours after transfection. qRT-PCR was used to determine the transfection efficiency of miR-27a.

Cell proliferation assay (CCK-8)

Transfected BMSCs were seeded into 96-well plates at a density of 5×103 cells per well, with five replicate wells per group. Blank wells containing only culture medium without cells were set for background correction. At 0, 24, 48, and 72 hours of culture, 10 μL of CCK-8 solution was added to each well and incubated for 2 hours. Absorbance (optical density, OD) at 450 nm was measured using a microplate reader to generate cell proliferation curves.

For background correction, the mean OD value of the blank wells was subtracted from the OD values of each experimental group to obtain corrected OD values. The experiment was repeated three times (three independent biological replicates), and cell proliferation curves were plotted based on the corrected OD values to evaluate the effect of miR-27a on BMSC proliferation.

Table 1. Comparison of relative expression levels of miR-27a and related genes in bone marrow tissue between the case group and the control group ($\bar{x}\pm s$).

Group	n	miR-27a	Runx2	BMP-2
Control group	80	1.02±0.11	1.00±0.10	0.99±0.10
Case group	80	0.35±0.07	0.42±0.05	0.38±0.07
t		45.962	46.400	44.697
P		< 0.001	< 0.001	< 0.001

Note: Runx2: Runt-related transcription factor 2; BMP-2: Bone morphogenetic protein 2.

ALP staining and activity assay

The osteogenic induction medium consisted of low-glucose DMEM supplemented with 10 mmol/L sodium β-glycerophosphate, 50 μg/mL ascorbic acid, and 10 nmol/L dexamethasone. Transfected BMSCs were seeded into 24-well plates at a density of 5×10^4 cells per well. After cell attachment, the culture medium was replaced with osteogenic induction medium to induce osteogenic differentiation.

After 7 days of induction, cells were stained using an ALP staining kit to qualitatively assess osteogenic differentiation under an inverted microscope. ALP activity in cell lysates was measured using an ALP activity assay kit to quantitatively evaluate osteogenic differentiation. Briefly, cells were collected and lysed with RIPA lysis buffer, total protein was extracted, and protein concentration was determined by the BCA method. ALP activity was expressed as units of enzyme activity per milligram of protein (U/mg) to quantitatively assess the degree of osteogenic differentiation. The experiment was repeated three times (three independent biological replicates), with three replicate wells per group in each experiment.

Alizarin red staining for calcium nodule formation

Transfected BMSCs were seeded into 24-well plates and cultured in the osteogenic induction medium described above for 14 days. The medium was then discarded, and the cells were washed three times with PBS and fixed with 4% paraformaldehyde for 30 minutes. Alizarin red staining was performed according to the instructions of the staining kit. Calcium nodule formation was observed and photographed under an inverted microscope.

Calcium nodule quantification was performed using ImageJ software. At a magnification of 100×, five fields of view were randomly selected from each well, and a uniform staining threshold was set. The number of red nodules with an area ≥50 μm^2 in each field of view was counted, and the mean value was taken as the number of calcium nodules in that well. Counting was performed in a blinded manner by two experimenters independently, and only consistent results were accepted. The experiment was repeated three times (three independent biological replicates), with three replicate wells per group in each experiment.

Statistical Analysis

Data were analyzed using SPSS 26.0 software. Measurement data are presented as mean ± standard deviation ($\bar{x}\pm s$). The Shapiro–Wilk test was first used to assess normality, and all data conformed to a normal distribution. Intergroup comparisons between two groups were performed using independent-samples t-tests, and comparisons among multiple groups were conducted using one-way ANOVA followed by LSD-t tests for pairwise comparisons. Pearson correlation analysis was used to assess the relationships between miR-27a and the expression levels of Runx2 and BMP-2. All cell experiments were independently repeated at least three times. A P-value <0.05 was considered statistically significant.

Results

Comparison of miR-27a and related gene expression levels in bone marrow tissue between the case and control groups

The relative expression level of miR-27a in bone marrow tissue was significantly lower in the case group than in the control group (P<0.001; Table 1). Pearson correlation analysis showed that miR-27a expression in bone marrow tissue from SAN patients was positively correlated with Runx2 expression (r=0.683, P<0.001) and positively correlated with BMP-2 expression (r=0.651, P<0.001).

Expression level of miR-27a in transfected BMSCs

Compared with the mimic NC group, the relative expression of miR-27a was significantly upregulated in the miR-27a mimic group [(0.98±0.07) vs (3.25±0.21), t=17.762, P<0.001], and was significantly downregulated in the miR-27a inhibitor group [(0.98±0.07) vs (0.28±0.05), t=13.219, P<0.001].

Effect of miR-27a on BMSC proliferation

At 24, 48, and 72 hours of culture, the OD values of the miR-27a mimic group were significantly higher than those of the mimic NC group (t=4.159, 5.765, 5.141; P=0.014,

Table 2. Comparison of OD values of BMSCs in each group at different time points ($\bar{x}$±s, n=3).

Group	0h	24h	48h	72h
mimic NC group	0.20±0.02	0.34±0.03	0.51±0.04	0.77±0.05
miR-27a mimic group	0.22±0.03	0.48±0.05*	0.75±0.06*	1.05±0.08*
miR-27a inhibitor group	0.21±0.02	0.25±0.03*	0.32±0.04*	0.45±0.05*

*Note: Compared with the mimic NC group, *P<0.05; n=3 represents three independent biological replicates; BMSCs: Bone marrow mesenchymal stem cells; NC: Negative control.*

Table 3. Comparison of osteogenic differentiation-related indicators in BMSCs among groups ($\bar{x}$±s, n=3).

Group	ALP activity (U/mg)	Number of calcium nodules (count)
mimic NC group	51.89±3.98	12.15±1.28
miR-27a mimic group	89.65±6.32*	25.32±2.15*
miR-27a inhibitor group	28.74±3.15*	5.32±0.85*

*Note: Compared with the mimic NC group, *P<0.05. n=3 represents three independent biological replicates; ALP: Alkaline phosphatase; BMSCs: Bone marrow mesenchymal stem cells; NC: Negative control.*

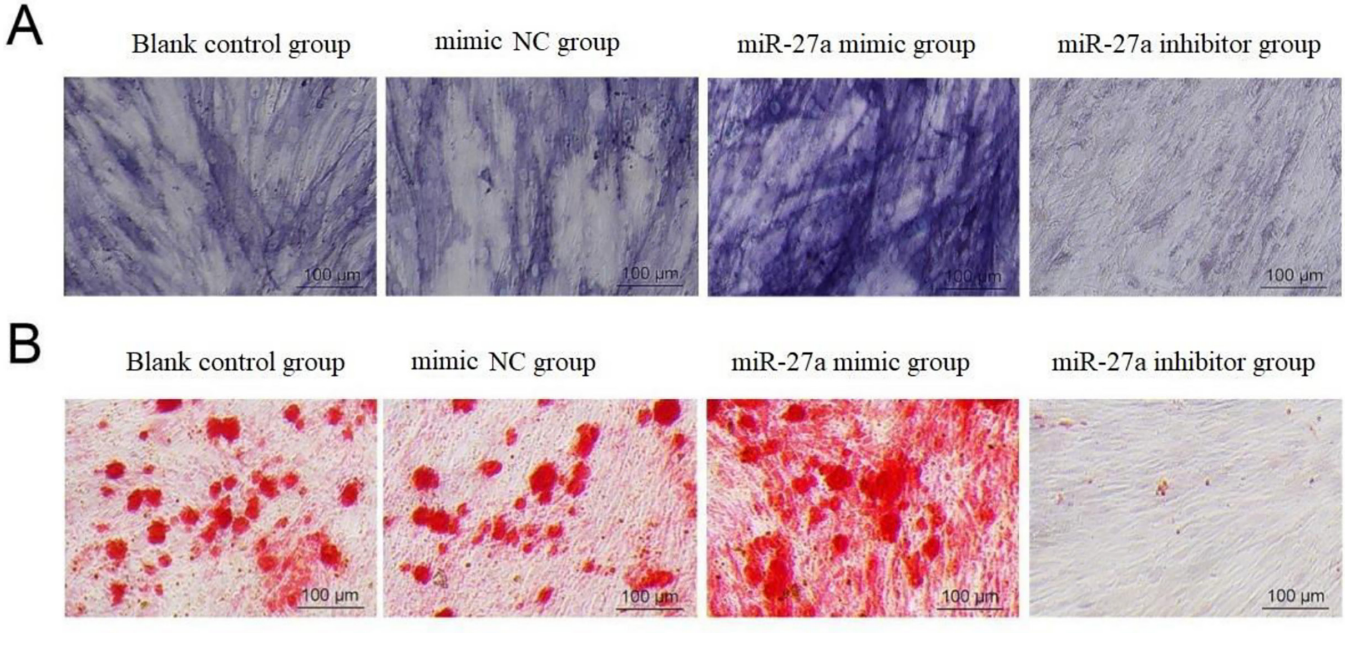

Figure 1. ALP and Alizarin Red S staining of BMSCs. Note: Groups from left to right are: Blank control group, mimic NC group, miR-27a mimic group, miR-27a inhibitor group. A: Representative images of ALP staining in BMSCs from each group after 7 days of osteogenic induction. B: Representative images of Alizarin Red S staining for calcium nodules in BMSCs from each group after 14 days of osteogenic induction (scale bar = 100 μm). The blank control group is shown for qualitative comparison only and was not included in quantitative statistical analyses. ALP: Alkaline phosphatase; BMSCs: Bone marrow mesenchymal stem cells; NC: Negative control.

Table 4. Comparison of relative expression levels of osteogenic-related genes in BMSCs among groups ($\bar{x}\pm s$, n=3).

Group	Runx2	BMP-2
mimic NC group	0.97±0.09	0.98±0.09
miR-27a mimic group	2.56±0.15*	2.32±0.12*
miR-27a inhibitor group	0.42±0.05*	0.38±0.06*

*Note: Compared with the mimic NC group, *P<0.05. n=3 represents three independent biological replicates; BMSCs: Bone marrow mesenchymal stem cells; NC: Negative control; Runx2: Runt-related transcription factor 2; BMP-2: Bone morphogenetic protein 2.*

<0.001, <0.001, respectively), and were significantly lower in the miR-27a inhibitor group at the same time points (t=3.464, 5.410, 7.318; P=0.026, 0.006, 0.002, respectively) (Table 2).

Effect of miR-27a on osteogenic differentiation of BMSCs

After 7 days of osteogenic induction, the miR-27a mimic group exhibited more intense ALP staining, significantly higher ALP activity, and a greater number of calcium nodules compared with the mimic NC group (t=9.116, P=0.001). After 7 days of osteogenic induction, the miR-27a inhibitor group showed weaker ALP staining than the mimic NC group. Quantitatively, ALP activity was significantly lower in the miR-27a inhibitor group (t=7.734, P=0.002), and the number of calcium nodules was also significantly reduced (t=7.987, P=0.001) (Table 3, Figure 1).

Effect of miR-27a on the expression of osteogenic-related genes in BMSCs

Compared with the mimic NC group, the relative expression levels of Runx2 and BMP-2 were significantly upregulated in the miR-27a mimic group (t=15.743 and 15.473, respectively; both P<0.001). In contrast, the relative expression levels of Runx2 and BMP-2 were significantly downregulated in the miR-27a inhibitor group compared with the mimic NC group (t=8.985 and 10.739, respectively; P=0.001 and P<0.001) (Table 4).

Discussion

The successful progression of bone repair relies on the normal proliferation and osteogenic differentiation potential of bone marrow mesenchymal stem cells (BMSCs). In steroid-associated femoral head osteonecrosis (SAN), glucocorticoid (GC)-induced functional abnormalities of BMSCs represent a key pathogenic mechanism, disrupting the balance between bone formation and repair[8]. This study focused on miR-27a to investigate its expression pattern and regulatory effects on BMSC function in SAN, with the aim of further elucidating the molecular mechanisms underlying the disease.

The regulatory roles of microRNAs (miRNAs) in SAN have been widely reported[9]. For example, miR-224-5p promotes bone formation in steroid-induced osteonecrosis models by targeting and inhibiting Smad4, and its expression is significantly upregulated in the bone marrow tissue of SAN patients[10]. miR-196b-5p enhances osteoclast activity by downregulating SIRT1, and its expression level is positively correlated with the severity of femoral head necrosis[11]. In addition, miR-21 has been shown to enhance BMSC proliferation by activating the PI3K/Akt pathway, but its expression is reduced in patients[12].

In this study, the relative expression level of miR-27a in the bone marrow tissue of SAN patients was significantly lower than that in the control group, which is consistent with the findings of Cui et al.[13]. The low expression of miR-27a may be a common molecular feature of SAN. Notably, the degree of miR-27a downregulation in this study (approximately 65.7%) was greater than the 42% reported by Cui et al. in animal models. This difference may be attributable to species differences; individual heterogeneity in clinical samples (such as cumulative steroid dose, duration of treatment, and ARCO stage); or differences in sampling site (in this study, bone marrow was collected from the necrotic area of the proximal femoral head, whereas in the animal model it was collected from femoral head tissue). The underlying mechanism is likely related to GC exposure: GCs can activate glucocorticoid receptors (GRs), which then bind to the promoter region of the miR-27a gene and inhibit its transcription[14].

Furthermore, correlation analysis in this study showed that miR-27a expression in bone marrow tissue from SAN patients was significantly and positively correlated with the expression levels of the osteogenic-related genes Runx2 and BMP-2. This result strengthens the link between miR-27a downregulation and osteogenic impairment at the clinical level and suggests that miR-27a may participate in the pathogenesis of SAN by regulating the expression of Runx2 and BMP-2.

The regulatory effect of miR-27a on BMSC proliferation was clearly demonstrated in this study. Our results showed that overexpression of miR-27a significantly enhanced

BMSC proliferative activity, whereas inhibition of miR-27a produced the opposite effect. This finding is consistent with previous studies on miRNA-mediated regulation of stem cell proliferation; for example, miR-875-5p promotes BMSC proliferation by targeting NOTCH3 to activate the Notch pathway[15], and miR-665 inhibits cell proliferation by downregulating SOST[16].

Mechanistically, miR-27a may exert its effects by targeting negative regulators of the cell cycle. In other disease models, such as differentiated thyroid cancer, miR-27a-5p has been reported to directly target the 3′UTR of SREBP1 and thereby modulate cell cycle progression and proliferation[17]. It is speculated that miR-27a may influence BMSC proliferation through a similar target gene regulatory mechanism, but this hypothesis requires further experimental validation.

Runx2, a core transcription factor for osteogenic differentiation, initiates the expression of osteoblast-specific genes and is often referred to as the "molecular switch" of bone formation[18]. BMP-2 activates the Smad1/5/8 pathway and acts synergistically with Runx2 to promote osteoblast differentiation and bone matrix mineralization, together forming a key regulatory axis for osteogenic differentiation[19]. In our study, the miR-27a mimic group exhibited significantly increased ALP activity and calcium nodule formation, accompanied by upregulated expression of Runx2 and BMP-2. Conversely, the miR-27a inhibitor group showed the opposite trends, which is consistent with the findings of Tang et al.[20]. These results suggest that miR-27a may enhance the osteogenic differentiation of BMSCs by upregulating the expression of these two genes.

However, it should be emphasized that this study did not directly validate Runx2 or BMP-2 as direct targets of miR-27a using luciferase reporter assays, nor can it confirm that the observed functional effects are mediated solely by these two genes. Therefore, the regulatory relationship between miR-27a and Runx2/BMP-2 in this study is based on correlations in expression and function, rather than a directly demonstrated regulatory pathway. Future research should clarify this issue through target gene validation experiments, and further explore whether miR-27a regulates BMSC function by modulating additional target genes or signaling pathways.

Limitations

This study has several limitations. 1) It adopted a single-center design, and the sample was limited to patients from our hospital, which may result in selection bias. The generalizability of the findings requires further verification in multicenter studies with larger sample sizes. 2) The *in vitro* experiments used commercially sourced BMSCs rather than BMSCs derived from SAN patients. Patient-derived cells may better reflect the biological characteristics of BMSCs under disease conditions, and functional differences between commercial and patient-derived cells may affect the clinical relevance of the conclusions. 3) Runx2 and BMP-2 were not directly validated as targets of miR-27a by luciferase reporter assays, and the specific downstream signaling pathways involved in this regulation were not clarified. 4) *In vivo* functional studies were not performed, so this study cannot confirm whether miR-27a regulates the progression of SAN in animal models. 5) In addition, bone marrow samples in the case group were collected from the necrotic proximal femoral head, whereas control samples were obtained from the iliac crest. Differences in anatomical site and local microenvironment may have influenced gene expression independently of SAN. These limitations should be addressed in future studies.

Conclusion

In summary, this study confirmed that miR-27a is downregulated in the bone marrow tissue of SAN patients and that its expression is positively correlated with the expression of the osteogenic genes Runx2 and BMP-2. *In vitro*, miR-27a enhanced the osteogenic differentiation capacity of BMSCs by promoting proliferation and upregulating Runx2 and BMP-2 expression. These findings highlight a potential role of miR-27a in the pathogenesis of SAN and provide preliminary experimental evidence supporting miR-27a as a candidate target for future molecularly targeted therapies in SAN.

Ethics approval

This study was approved by the Ethics Committee of The Third Central Hospital of Tianjin (approval ID: SZX-IRB-SOP-016(F)-002-08) and was conducted in accordance with the Declaration of Helsinki (1964) and its later amendments.

Consent to participate

Written informed consent was obtained from all participants.

Authors' contributions

ZC, JM, and MW designed the study and drafted the manuscript. ZZ, MW, and YC were responsible for the collection and analysis of experimental data. SL, JM, CZ, and SG critically revised the manuscript for important intellectual content. All authors read and approved the final version of the manuscript.

References

1. Li L, Zhao S, Leng Z, Chen S, Shi Y, Shi L, Li J, Mao K, Tang H, Meng B, Wang Y, Shang G, Liu H. Pathological mechanisms and related markers of steroid-induced osteonecrosis of the femoral head. Ann Med. 2024;56(1):2416070.
2. Huang C, Qing L, Xiao Y, Tang J, Wu P. Insight into Steroid-Induced ONFH: The Molecular Mechanism and Function of Epigenetic Modification in Mesenchymal Stem Cells. Biomolecules. 2023;14(1):4.
3. Yang W, Pan Q, Peng Y, Hu Y, Cui Y, Shao Z, Meng C, Wang H, Huang W. Dual-target nanotherapy for

vascular endothelium and bone mesenchymal stem cells halt steroid-induced osteonecrosis of the femoral head progression. J Control Release. 2025;380:219-239.
4. Tang B, Chen Y, Zhao P, Yan W, Huang X, Jiang W, Sun M, Zhang H, Xiang D, Chen T, Lian C, Zhang J. MiR-601-induced BMSCs senescence accelerates steroid-induced osteonecrosis of the femoral head progression by targeting SIRT1. Cell Mol Life Sci. 2023;80(9):261.
5. Huang X, Jie S, Li W, Li H, Ni J, Liu C. miR-122-5p targets GREM2 to protect against glucocorticoid-induced endothelial damage through the BMP signaling pathway. Mol Cell Endocrinol. 2022;544:111541.
6. Bi W, Li J, Xiong M, Pan B, Zhang Z, Nasifu L, He B, Wang P. The diagnostic and prognostic role of miR-27a in cancer. Pathol Res Pract. 2023;247:154544.
7. Zeng Z, Fei L, Yang J, Zuo J, Huang Z, Li H. MiR-27a-3p Targets GLP1R to Regulate Differentiation, Autophagy, and Release of Inflammatory Factors in Pre-Osteoblasts via the AMPK Signaling Pathway. Front Genet. 2022;12:783352.
8. Zhang J, Cao J, Liu Y, Zhao H. Advances in the Pathogenesis of Steroid-Associated Osteonecrosis of the Femoral Head. Biomolecules. 2024;14(6):667.
9. Zuo R, Cao B, Kong L, Wang F, Li S, Shan H, Guan J, Kang Q. MiR-370-3p regulate TLR4/SLC7A11/GPX4 to alleviate the progression of glucocorticoids-induced osteonecrosis of the femoral head by promoting osteogenesis and suppressing ferroptosis. J Orthop Translat. 2025;51:337-358.
10. Cao Y, Jiang C, Wang X, Wang H, Yan Z, Yuan H. Reciprocal effect of microRNA-224 on osteogenesis and adipogenesis in steroid-induced osteonecrosis of the femoral head. Bone. 2021;145:115844.
11. Xie Y, Zhou J, Tian L, Dong Y, Yuan H, Zhu E, Li X, Wang B. miR-196b-5p Regulates Osteoblast and Osteoclast Differentiation and Bone Homeostasis by Targeting SEMA3A. J Bone Miner Res. 2023;38(8):1175-1191.
12. Lv C, Yang S, Chen X, Zhu X, Lin W, Wang L, Huang Z, Wang M, Tu G. MicroRNA-21 promotes bone mesenchymal stem cells migration *in vitro* by activating PI3K/Akt/MMPs pathway. J Clin Neurosci. 2017;46:156-162.
13. Cui Y, Huang T, Zhang Z, Yang Z, Hao F, Yuan T, Zhou Z. The potential effect of BMSCs with miR-27a in improving steroid-induced osteonecrosis of the femoral head. Sci Rep. 2022;12(1):21051.
14. Tang J, Yu H, Wang Y, Duan G, Wang B, Li W, Zhu Z. miR-27a promotes osteogenic differentiation in glucocorticoid-treated human bone marrow mesenchymal stem cells by targeting PI3K. J Mol Histol. 2021;52(2):279-288.
15. Tang Z, Zhang W, Liu A, Wei C, Bai M, Zhao J, Wang J. Circ_0104873 promotes osteoarthritis progression via miR-875-5p/NOTCH3/Notch signaling pathway. Int J Biol Macromol. 2024;281(Pt 1):136175.
16. Zeng X, Yuan X, Liao H, Wei Y, Wu Q, Zhu X, Li Q, Chen S, Hu M. The miR-665/SOST Axis Regulates the Phenotypes of Bone Marrow Mesenchymal Stem Cells and Osteoporotic Symptoms in Female Mice. Am J Pathol. 2024;194(11):2059-2075.
17. Xie Z, Liu J, Zhou J, Zhang X, Li Z. MiR-27a-5p inhibits malignant progression of differentiated thyroid cancer by directly affecting the miR-27a-5p/SREBP1 axis. J Endocrinol Invest. 2025;48(6):1317-1331.
18. Komori T. Regulation of Skeletal Development and Maintenance by Runx2 and Sp7. Int J Mol Sci. 2024;25(18):10102.
19. Zhang Q, Long Y, Jin L, Li C, Long J. Non-coding RNAs regulate the BMP/Smad pathway during osteogenic differentiation of stem cells. Acta Histochem. 2023;125(1):151998.
20. Tang JS, Yu HX, Ruan RX, Chen R, Zhu ZQ. LncRNA SNHG14 Delivered by Bone Marrow Mesenchymal Stem Cells-Secreted Exosomes Regulates Osteogenesis and Adipogenesis in Osteoporosis by Mediating the miR-27a-3p/LMNB1 Axis. Kaohsiung J Med Sci. 2025;41(5):e70004.